Monatsh Chem
DOI 10.1007/s00706-016-1906-4

ORIGINAL PAPER

Synthesis and characterization of DETA/Cu(NO_3)$_2$ supported on magnetic nanoparticles: a highly active and recyclable catalyst for the solvent-free synthesis of polyhydroquinolines

Lotfi Shiri[1] · **Arash Ghorbani-Choghamarani**[1] · **Mosstafa Kazemi**[1]

Received: 6 August 2016 / Accepted: 30 December 2016

Abstract A new magnetically separable catalyst consisting of Cu(II) complex immobilized on Fe_3O_4 nanoparticles functionalized with diethylenetriamine (Fe_3O_4–DETA–Cu(II)) was successfully synthesized and characterized by FT-IR, SEM, EDS, VSM, TGA, XRD, and AAS techniques. This synthesized nanosolid was shown to be an efficient heterogeneous catalyst for the solvent-free synthesis of polyhydroquinoline derivatives. The catalyst was readily separated from the final product solution by magnetic decantation and reused for subsequent reactions for at least seven runs with less deterioration in catalytic activity.

Graphical abstract

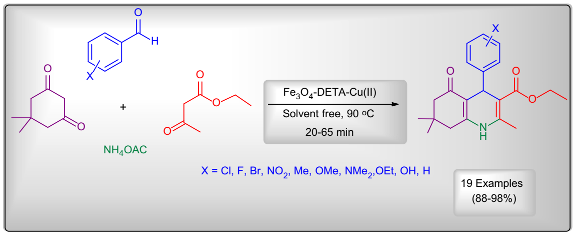

Keywords Heterogeneous catalysis · Magnetically separable catalyst · Polyhydroquinoline · Solvent-free

Introduction

Nowadays, search for finding separable and reusable catalysts become a hot research topic in chemistry, especially in modern catalysis research. The immobilization of homogeneous catalysts on heterogeneous supports is in fact an efficient strategy to reach this goal [1]. In recent times, compared to the conventional separation, magnetic separation has emerged as a robust, highly efficient, easy, and rapid separation technique for products and catalysts [2]. The catalyst supported on magnetic nanoparticles (MNPs) can be readily separated from the reaction media using an external magnet, without the need for filtration, centrifugation, or other tedious workup processes [3, 4]. In addition, magnetic-supported catalysts can be reused many times while keeping their initial activity. Among the various employed magnetic NPs as the core magnetic support, Fe_3O_4 nanoparticles have been widely studied both for their scientific interests and technological applications [5].

The designing and developing of copper-catalyzed routes for organic reactions is a hot research topic in modern catalysis research, because compared to other transition metals, copper is less toxic, available, and inexpensive [6]. In recent times, copper complex immobilized on magnetic Fe_3O_4 nanoparticles has been recognized as an efficient catalytic strategy for a range of organic reactions, such as carbon–carbon and carbon–heteroatom bonds formation, oxidation and multi-component reactions [4–7].

Heterocyclic compounds, especially nitrogen-containing heterocycles, have attracted profound attention in modern chemistry science because they play a key role in the fields of natural products, medicinal chemistry and materials chemistry. In recent times, a lot of attention has been focused on the synthesis of polyhydroquinoline derivatives, because

---

Electronic supplementary material The online version of this article (doi:10.1007/s00706-016-1906-4) contains supplementary material, which is available to authorized users.

✉ Lotfi Shiri
lshiri47@gmail.com

[1] Department of Chemistry, Faculty of Basic Sciences, Ilam University, P.O. Box 69315-516, Ilam, Iran

they are well-known as Ca^{2+} channel blockers, and have emerged as an important class of drugs for the treatment of cardiovascular diseases [8]. In fact, cardiovascular agents, such as nifedipine, nicardipine, amlodipine (Fig. 1) are effective dihydropyridine drugs for the treatment of hypertension [9]. Polyhydroquinolines and their derivatives also possess a variety of biological and pharmaceutical activities, such as antidiabetic, hepatoprotective, vasodilator, geroprotective, antiatherosclerotic, bronchodilator, anticancer, and antitumor activities [10–12]. In chemistry, the dihydropyridine skeleton has been widely utilized as a hydride source for reductive amination [9]. The classical procedure for the synthesis of polyhydroquinolines is the one-pot condensation of aldehydes with 1,3-dicarbonyl compounds and ammonia either in acetic acid or refluxing in alcohol [13]. In general, traditional procedures are unpleasant from the economic and environment points of view. In this respect, during the last decade, new strategies toward the synthesis of dihydroquinolines have been focused on a catalytic version. For example, for the synthesis of polyhydroquinolines, a variety of catalysts, such as ionic liquid [14], TMSCl-NaI [15], heteropoly acid [16], sulfamic acid [2], nickel nanoparticle [17], MCM-41 [18], $ZrCl_4$ [19], and *p*-TSA [20] have been recently reported in the literature. Most of these protocols suffer from some drawbacks, such as requiring large amount of the catalyst and toxic solvents, product contamination, formation of by-products, long reaction times, difficulty in catalyst separation from the reaction media and recycling which is a serious problem in the pharmaceutical industry. Therefore, the search for improving reaction conditions for the synthesis of polyhydroquinoline derivatives using efficient and reusable catalysts under solvent-free conditions is a prime and real challenge for synthetic chemists. Now, in this paper, we report a highly efficient and eco-friendly multi-component protocol for the synthesis of polyhydroquinolines using Fe_3O_4–DETA–Cu(II) as a magnetically recoverable catalyst under solvent-free conditions.

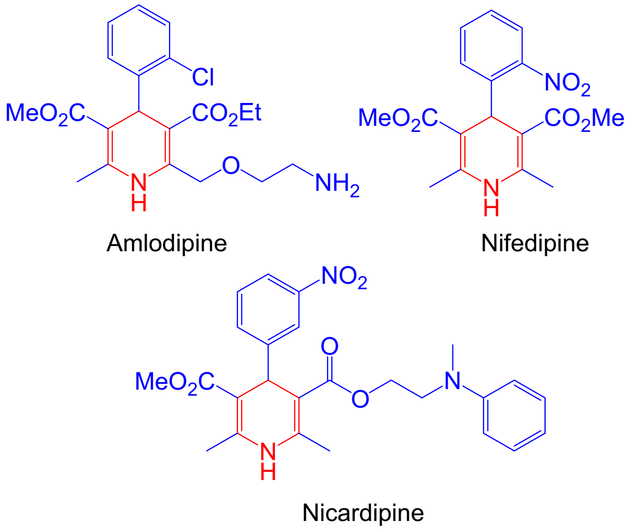

Fig. 1 Typical dihydropyridine drugs

Result and discussion

Preparation and characterization of Fe_3O_4–DETA–Cu(II)

Magnetic Fe_3O_4 nanoparticles supported-DETA/Cu(II) was successfully synthesized using the surface modification strategy as depicted in Scheme 1. The magnetic nanoparticles (Fe_3O_4 MNPs) were prepared by chemical co-precipitation method [21] and coated with 3-chloropropyltrimethoxysilane (CPTMS) by covalent bonds [22]. The reaction of the supported CPTMS with diethylenetriamine (DETA) in toluene under reflux conditions for 42 h produced the DETA functionalized Fe_3O_4 nanoparticles (Fe_3O_4–DETA). Finally, the Fe_3O_4–DETA treated with $Cu(NO_3)_2 \cdot 3H_2O$ in ethanol at reflux temperature for 24 h to provide magnetic nanoparticles supported-DETA/Cu(II).

The prepared magnetic nanocatalyst was comprehensively characterized by FT-IR, TGA, XRD, SEM, EDS, AAS, and VSM analysis techniques. The FT-IR spectra for the Fe_3O_4 MNPs (a), Fe_3O_4–CPTMS (b), Fe_3O_4–DETA (c), and Fe_3O_4–DETA–Cu(II) (d) are displayed in Fig. 2. The FT-IR analysis of the Fe_3O_4 MNPs exhibits a characteristic peak at 579 cm^{-1}, which is attributed to the Fe–O stretching vibration. Also, the broad band at around 3400 cm^{-1} is attributed to bound water O–H stretching vibration adsorption. The anchored CPTMS on Fe_3O_4 MNPs is confirmed by a characteristic peak at 996 cm^{-1}, which is attributed to Fe–O–Si stretching vibration. In the curve of Fe_3O_4–DETA, three obvious peaks at 1040, 1119, and 1203 cm^{-1} are proved the existence of C–N bonds and their vibration. FT-IR spectrum of the Fe_3O_4–DETA–Cu(II) catalyst showed two characteristic peaks at 1621 and 3432 cm^{-1}, which are corresponded to N–H bending and stretching mode, respectively. Therefore, it can be concluded that Cu(II) complex was immobilized successfully on the surface of Fe_3O_4–DETA nanoparticles.

The morphology and size of the catalyst was studied by scanning electron microscope (SEM) as shown in Fig. 3. The SEM image of Fe_3O_4–DETA–Cu(II) shows that the catalyst was formed of nanometer-sized particles. The components of Fe_3O_4–DETA–Cu(II) were analyzed using energy-dispersive X-ray spectroscopy (EDS) (Fig. 4). As shown in Fig. 4, characteristic peaks of Fe, O, Si, C, N, and Cu demonstrated clearly that the copper(II) complex successfully immobilized on the surface of Fe_3O_4–DETA

Scheme 1

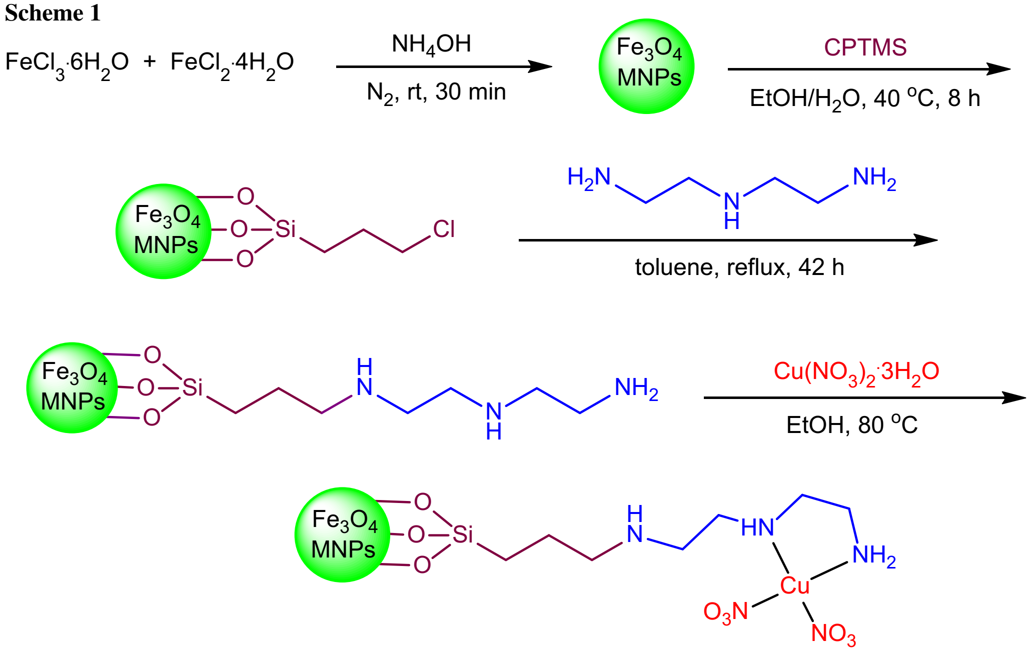

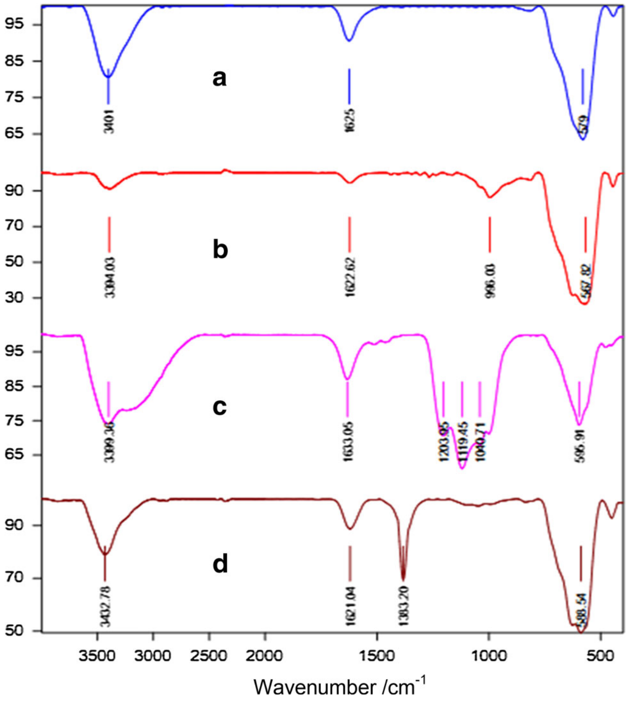

Fig. 2 FT-IR spectra of Fe_3O_4 MNPs (*a*), Fe_3O_4–CPTMS (*b*), Fe_3O_4–DETA (*c*), and Fe_3O_4–DETA–Cu(II) (*d*)

nanoparticles. As a result of this analysis, the Fe_3O_4–DETA–Cu(II) catalyst has been successfully synthesized.

The magnetic property of the nano-magnetic catalyst was investigated by vibrating sample magnetometer (VSM) at ambient temperature. Figure 5 exhibits the magnetization curves of Fe_3O_4 MNPs and Fe_3O_4–DETA–Cu(II). It can be seen that the saturation of the obtained catalyst decreases from 55.1 to 38.25 emu g^{-1} for the Fe_3O_4 MNPs. The decrease of the saturation magnetization can be related to the presence of amine groups on the surface of the Fe_3O_4 nanoparticles supports. As a result of this analysis, the superparamagnetic properties of the prepared Fe_3O_4–DETA–Cu(II) are attractive for their application.

The TGA was used to determine the percent of functional groups chemisorbed onto the surface of magnetic nanoparticles. Figure 6 shows the TGA curves for bare Fe_3O_4 MNPs (red line), DETA-Fe_3O_4 (green line), and Fe_3O_4–DETA–Cu(II) (blue line). The TGA curve of the all samples shows the small amount of weight loss below 200 °C is due to desorption of physically adsorbed solvents and surface hydroxyl groups. Organic groups have been reported to desorb at temperatures above 260 °C. The organic groups on the DETA-Fe_3O_4 are found to have a mass percentage loss about 9%, while the Fe_3O_4–DETA–Cu(II) catalyst have greater mass loss, at about 32.5%. As a result of this analysis, it can be concluded that the well grafting of Cu(II) complex on the Fe_3O_4–DETA is verified.

X-ray diffraction (XRD) is an effective spectra technique to the better reorganization of the major properties of the magnetite structures. In fact, the formation of magnetite crystal phase in the nano-magnetic catalyst in aggregate powder form can be as well identified by the X-ray diffraction (XRD). The XRD-diffraction patterns of Fe_3O_4–DETA (green line or a), Fe_3O_4–DETA–Cu(II) (red line or b) and the recovered catalyst after seven cycles (blue line or c) are presented in Fig. 7. As seen in Fig. 7,

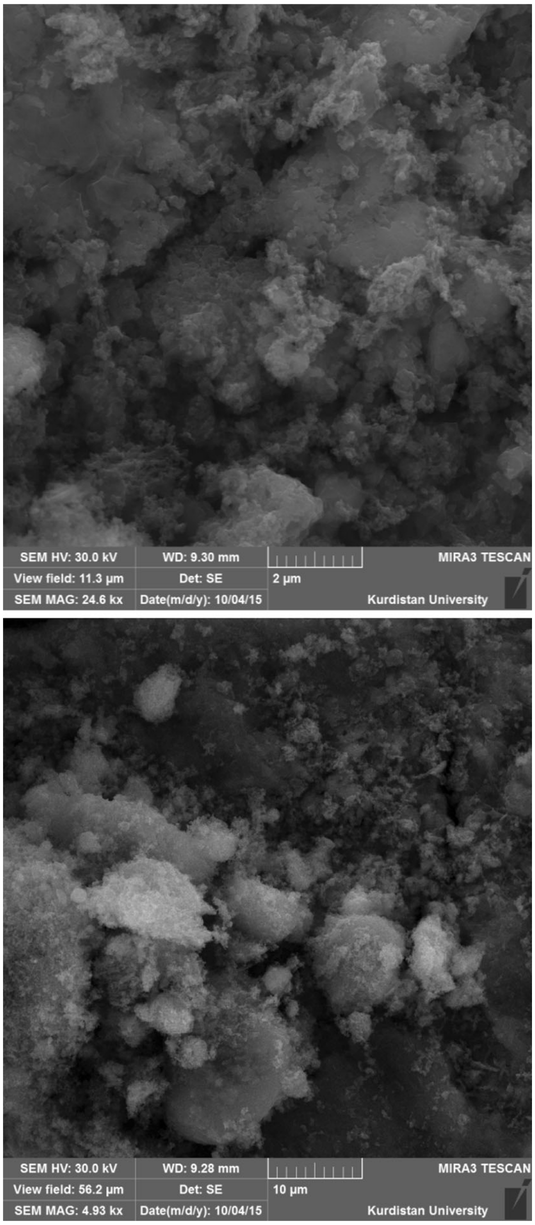

Fig. 3 SEM images of the Fe_3O_4–DETA–Cu(II)

several characteristic peaks at $2\theta = 34.5°$, 41.2°, 50.7°, 63.2°, 67.3°, and 74.5° were observed in all samples (Fig. 6a–c), which are related to the (220), (311), (400), (422), (511), and (440) planes of Fe_3O_4 nanoparticles with cubic phase (in good agreement with the standard Fe_3O_4 XRD spectrum reported in the literature) [6]. As shown in Fig. 6b, c, XRD-diffraction pattern of the recovered catalyst after seven times was nearly similar to the fresh catalyst. As a result of this analysis, the Fe_3O_4–DETA–Cu(II) catalyst had been synthesized successfully without damaging the crystal structure of Fe_3O_4 core.

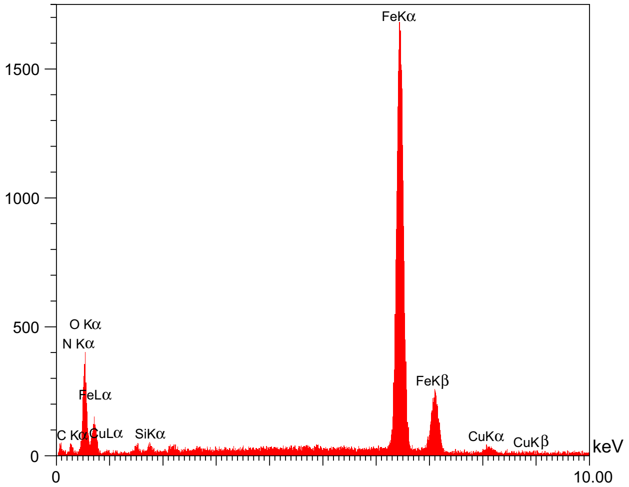

Fig. 4 EDS spectrum of the Fe_3O_4–DETA–Cu(II)

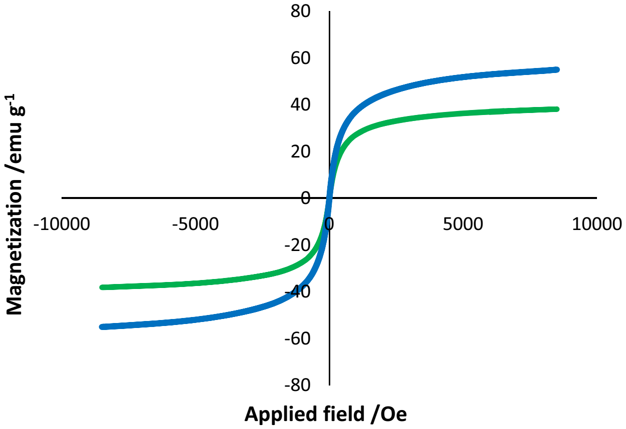

Fig. 5 Magnetization curves for Fe_3O_4 NPs (*blue line*) and Fe_3O_4–DETA–Cu(II) (*green line*) at room temperature

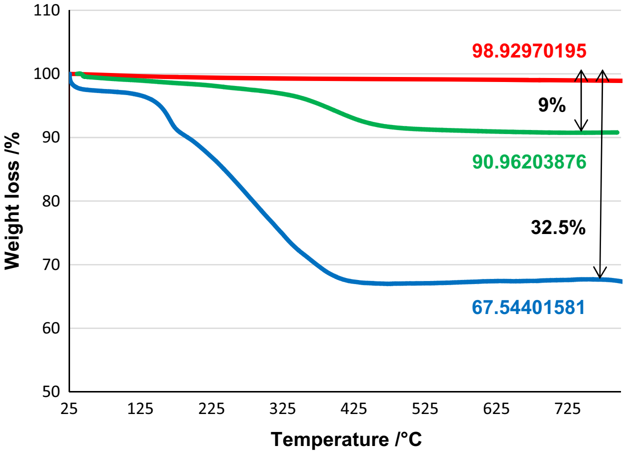

Fig. 6 TGA curves of Fe_3O_4 MNPs (*red line*), Fe_3O_4–DETA (*green line*), and Fe_3O_4–DETA–Cu(II) (*blue line*)

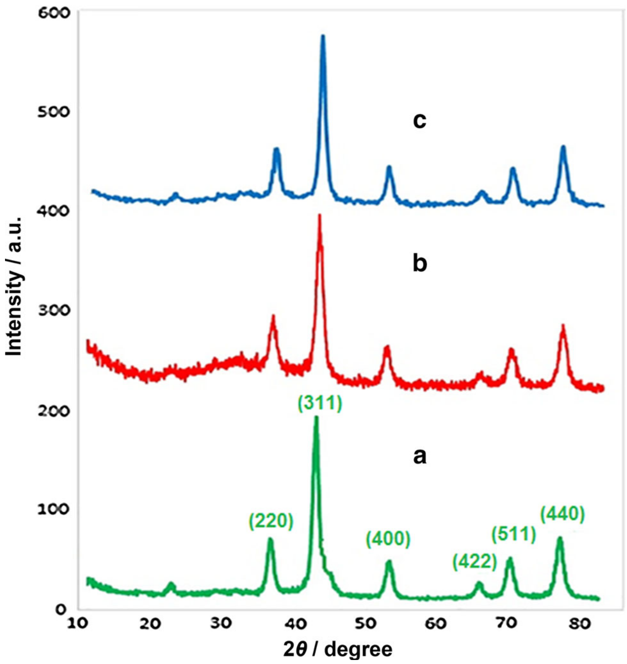

Fig. 7 The XRD patterns of Fe$_3$O$_4$–DETA (*a*), the fresh copper catalyst (*b*), the recovered copper catalyst after seven times (*c*)

Atomic absorption spectroscopy (AAS) of the fresh catalyst showed that the amount of copper loaded on the surface of Fe$_3$O$_4$ nanoparticles was about 0.15 mmol g^{-1}.

All together, these analyses are indicative of the successful immobilization of Cu(NO$_3$)$_2$ groups onto the amino-functionalized magnetite Fe$_3$O$_4$ nanoparticles.

Catalytic study

After successful characterization of the catalyst, we decided to evaluate the efficiency of the Fe$_3$O$_4$–DETA–Cu(II) in the synthesis of polyhydroquinolines. The control experiment and the optimization of the reaction condition were tested by choosing the reaction of 4-cholorobenzaldehyde (1 mmol), with ethyl acetoacetate (1 mmol), dimedone (1 mmol), and ammonium acetate (1.2 mmol) as model reaction. The reaction conditions were optimized by evaluating various parameters, such as catalyst concentration, solvent type, and temperature. The collected results from these experiments are listed in Table 1. In initial investigation, the effect of catalyst loading (from 4.5×10^{-2} mol% to 3×10^{-1} mol%) on the model reaction was screened in the absence of solvent at 90 °C (Table 1, entries 1–5). As can be seen from the summarized results in Table 1, the excellent yield of 98% was obtained when only 2.25×10^{-1} mol% of the copper catalyst was used. Further increase in catalyst concentration (3×10^{-1} mol%) does not show any significant effect on reaction time and yield of product (entry 5). Hence, 2.25×10^{-1} mol% of the catalyst was considered as an optimum catalyst concentration.

To identify the ideal solvent, the reaction furnishing **5a** was studied in several solvent (such as CH$_3$CN, THF, acetone, H$_2$O, EtOH, and H$_2$O/EtOH) at reflux temperature (Table 1, entries 6–11). The reaction in THF and water only gave product in low yields of 65 and 35%, respectively (entries 7 and 9). When the reaction was performed in CH$_3$CN, acetone, and H$_2$O/EtOH (entries 6, 8, and 11), respectively, the yields were slightly inferior to the results in EtOH (entry 10). Although the obtained results for EtOH were satisfactory and venerable, but the solvent-free method was found to be superior in terms of reaction time and product yield. Next, to evaluate the effect of temperature on the reactivity, the model reaction was carried out at various temperatures (Table 1, entries 12–14). As shown in Table 1, reaction times and yields of product **5a** were improved as the reaction temperature increased. However, no significant improvement on the yield was observed when the reaction performed at 100 °C (entry 14).

Finally, control experiments show that only a trace amount of the product was obtained in the absence of the copper catalyst after 120 min (Table 1, entry 15). Accordingly, as evident from Table 1, the best results for the product **5a** were obtained with 2.25×10^{-1} mol% of the catalyst under solvent-free conditions at 90 °C (entry 4).

To evaluate the scope and generality of this catalytic system, various aldehydes were used and converted to the polyhydroquinolines under the optimum conditions (Scheme 2). The results of this study are listed in Table 2. As shown in Table 2, a broad spectrum of aromatic aldehydes bearing electron-deficient or electron-rich substituents on the aromatic ring in the *ortho*, *meta*, and *para* positions were successfully subjected to the same reaction and the corresponding 1,4-DHP derivatives were obtained in admirable yields in satisfactory times. It is noteworthy that the kind of aldehyde has no significant effect on the reaction, because the desired products were obtained in high yields in relatively short reaction times.

To show the merits of this catalytic system in comparison with other reported protocols in the literature, we summarized the results for the preparation of product **5a** (as a model substrate) in Table 3. As shown in Table 3, this synthetic protocol is superior to some of the previously reported procedures in terms of product yield and reaction time. Furthermore, this new nano-magnetic catalyst is also comparable in terms of price, non-toxicity, stability, and easy separation.

The recovery and reusability of catalyst is an important aspect in catalytic processes. In this respect, the reusability of the Fe$_3$O$_4$–DETA–Cu(II) as catalyst in the model reaction was checked. After completion of the reaction, the

Table 1 Optimization of the reaction conditions

Entry	Catalyst/mol%	Solvent	Temperature/°C	Time/min	Yield/%[a]
1	4.5×10^{-2}	Solvent-free	90	70	78
2	7.5×10^{-2}	Solvent-free	90	50	84
3	1.5×10^{-1}	Solvent-free	90	35	95
4	2.25×10^{-1}	Solvent-free	90	20	98*
5	3×10^{-1}	Solvent-free	90	20	98
6	2.25×10^{-1}	CH_3CN	Reflux	180	85
7	2.25×10^{-1}	THF	Reflux	220	65
8	2.25×10^{-1}	Acetone	Reflux	190	80
9	2.25×10^{-1}	H_2O	Reflux	240	35
10	2.25×10^{-1}	EtOH	Reflux	150	90
11	2.25×10^{-1}	H_2O/EtOH(1:1)	80	165	82
12	2.25×10^{-1}	Solvent-free	70	60	92
13	2.25×10^{-1}	Solvent-free	80	35	95
14	2.25×10^{-1}	Solvent-free	100	20	97
15	–	Solvent-free	90	120	Trace

Reactions conditions: aldehyde (1 mmol), dimedone (1 mmol), ethyl acetoacetate (1 mmol), and ammonium acetate (1.2 mmol)

* Best reaction condition

[a] Isolated yield

Scheme 2

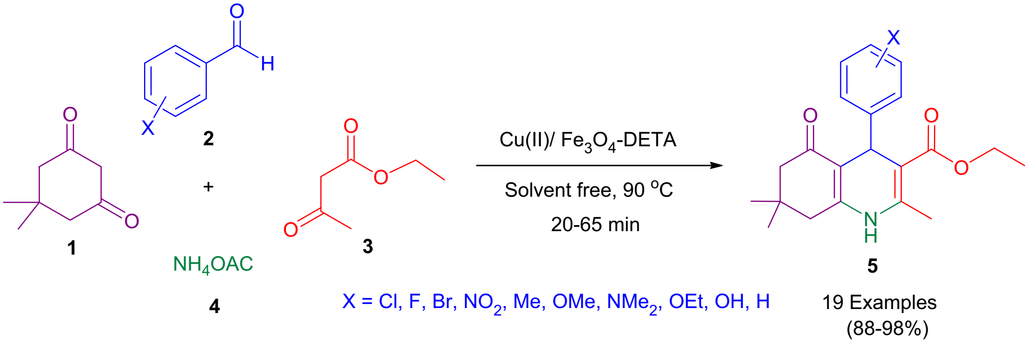

catalyst was separated easily and rapidly from the product by exposure to an external magnet, and the reaction solution was decanted magnetically. The remaining nanomagnetic catalyst was washed several times with ethyl acetate and dried to remove residual product, and subjected to the next run. The convenient separation using this strategy minimizes the loss of catalyst during separation. The recovered catalyst was used for seven successive times without any significant loss of its catalytic efficiency (Fig. 8). This reusability exhibits the high stability of the catalyst under the operating conditions.

To investigate the copper leaching in this reaction, the recovered catalyst was analyzed by AAS technique. The elemental analysis of the recovered catalyst after seven times by AAS indicated that the content of copper is about 0.13 mmol g^{-1}. AAS analysis revealed that the recovered catalyst did not show significant leaching and the reaction was truly heterogeneous in nature.

Also, the SEM image of the recovered catalyst is shown in Fig. 9. From the comparison of Fig. 9 with Fig. 3, it can be concluded that there is no significance difference in the morphologies of freshly prepared catalyst and the recovered catalyst after operation for seven consecutive reaction cycles.

Conclusion

In summary, DETA/Cu(II) immobilized on Fe_3O_4 nanoparticles was found to be an efficient and recoverable heterogeneous catalyst for the thermal solvent-free synthesis of polyhydroquinolines via the four-component

Table 2 Fe_3O_4–DETA–Cu(II) catalyzed the synthesis of polyhydroquinolines at 90 °C under solvent-free conditions

Entry	Aldehyde	Product	Time/min	Yield/%[a]	M.p./°C [References]
1	4-ClC_6H_4CHO	**5a**	20	98	238–240 [23]
2	4-$MeOC_6H_4CHO$	**5b**	30	94	250–252 [24]
3	4-MeC_6H_4CHO	**5c**	35	90	253–255 [23]
4	4-FC_6H_4CHO	**5d**	30	92	181–183 [25]
5	4-$O_2NC_6H_4CHO$	**5e**	40	91	240–242 [24]
6	4-BrC_6H_4CHO	**5f**	30	98	250–253 [23]
7	4-HOC_6H_4CHO	**5g**	55	93	232–234 [25]
8	4-$(Me)_2NC_6H_4CHO$	**5h**	45	97	232–234 [25]
9	4-$EtOC_6H_4CHO$	**5i**	35	95	178–180 [26]
10	C_6H_5CHO	**5j**	50	96	216–218 [25]
11	3-ClC_6H_4CHO	**5k**	30	94	232–234 [27]
12	3-$O_2NC_6H_4CHO$	**5l**	40	92	175–177 [24]
13	3-BrC_6H_4CHO	**5m**	35	95	233–235 [25]
14	3-OHC_6H_4CHO	**5n**	65	88	217–219 [27]
15	2-$O_2NC_6H_4CHO$	**5o**	40	89	209–211 [28]
16	2-ClC_6H_4CHO	**5p**	35	92	207–209 [29]
17	2-$MeOC_6H_4CHO$	**5q**	30	93	255–257 [30]
18	3,4-$(MeO)_2C_6H_3CHO$	**5r**	25	94	203–205 [24]
19	2,4-$(Cl)_2C_6H_3CHO$	**5s**	35	92	241–242 [23]

[a] Isolated yield

Table 3 Comparison of the activity of various catalysts in the synthesis of product **5a**

Entry	Catalyst	Condition	Time/min	Yield/%	References
1	GSA@MNPs	EtOH, reflux	200	94	[31]
2	$PdCl_2$	THF, reflux	240	87	[10]
3	$K_7[PW_{11}CoO_{40}]$	CH_3CN, reflux	30	80	[32]
4	$Hf(NPf_2)_4$	$C_{10}F_{18}$, 60 °C	120	96	[33]
5	Cu-SPATB/Fe_3O_4	PEG-400, 80 °C	65	98	[21]
6	$[TBA]_2[W_6O_{19}]$	Solvent-free, 110 °C	20	95	[34]
7	Fe_3O_4–DETA–Cu(II)	Solvent-free, 90 °C	20	98	This work

reaction of aromatic aldehydes with ethyl acetoacetate, dimedone, and ammonium acetate. Notably, a broad spectrum of polyhydroquinoline derivatives was obtained in admirable yields. The nanosolid catalyst was readily separated from the final product solution by magnetic decantation and reused for seven times with only minimal reduction in the catalytic activity. This catalytic system suggests a series of significant advantages, such as easy separation by external magnetic field, solvent-free conditions, high product yields and simplicity of operation. As a result of this study, this catalytic system can act as an efficient strategy for the synthesis of biologically and pharmaceutically active molecules.

Experimental

Chemicals were purchased from Fisher and Merck. The reagents and solvents used in this work were obtained from Sigma-Aldrich, Fluka, or Merck and used without further purification. The particles size and morphology were investigated by a JEOL JEM-2010 scanning electron microscopy (SEM), on an accelerating voltage of 200 kV. IR spectra were recorded as KBr pellets on a VRTEX 70 model BRUKER FT-IR spectrophotometer. Powder XRD was collected with a Rigaku-Dmax 2500 diffractometer with nickel filtered Cu Kα radiation ($\lambda = 1.5418$ Å, 40 kV). Thermogravimetric analysis (TGA) curves were

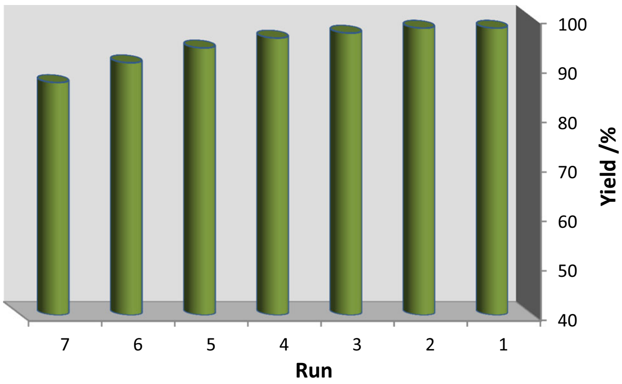

Fig. 8 Reusability of Fe_3O_4–DETA–Cu(II) in the synthesis of product **5a**

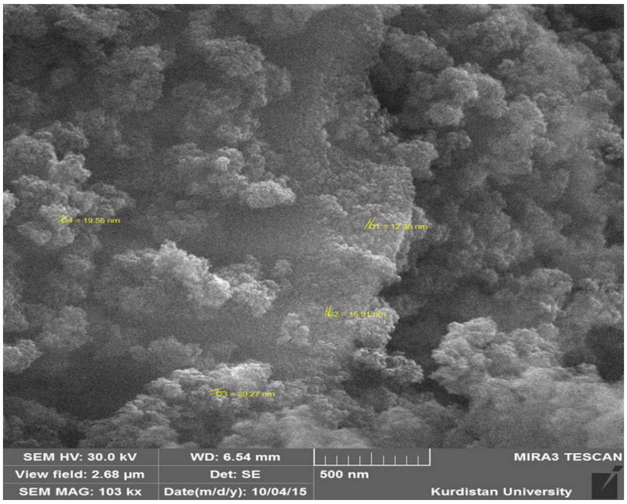

Fig. 9 SEM image of the recovered catalyst (Fe_3O_4–TBA–Br_3) after seven runs

recorded using a PL-STA 1500 device manufactured by Thermal Sciences. The magnetic property of Fe_3O_4 nanoparticles and the catalyst was characterized by vibrating sample magnetometer (VSM, MDKFD, Iran). The concentration of the copper in the catalyst was measured using an atomic absorption spectrophotometer (AAS) (UV/Vis, Analytikjena, nova-400p, Germany).

Preparation of the magnetic Fe_3O_4-nanoparticles

The mixture of 5.838 g $FeCl_3 \cdot 6H_2O$ (0.0216 mol) and 2.147 g $FeCl_2 \cdot 4H_2O$ (0.0108 mol) was dissolved in 100 cm^3 of deionized water in a three-necked flask (250 cm^3) under N_2 atmosphere. After that, under rapid mechanically stirring, 10 cm^3 of ammonia solution was added into the solution within 30 min with vigorous mechanical stirring. After being rapidly stirred for 30 min, the resultant black dispersion was heated to 80 °C for 30 min. The black precipitate formed was isolated by magnetic decantation, washed with double-distilled water until neutrality, and further washed twice with ethanol and dried at room temperature.

Preparation Fe_3O_4–CPTMS

The obtained Fe_3O_4 nanoparticles (1.5 g) was dispersed in 250 cm^3 ethanol/water (volume ratio, 1:1) by sonication for 30 min, and then 2 cm^3 CPTMS was added to the mixture reaction. The reaction mixture was stirred using mechanically stirring under N_2 atmosphere at 40 °C for 8 h. Then, the nanoparticles was re-dispersed in ethanol by sonication for 5 times and separated through magnetic decantation. The nanoparticles product (Fe_3O_4–CPTMS) was dried at room temperature.

Preparation of Fe_3O_4–DETA

The *N*-propylcholoro-functionalized Fe_3O_4 (1.5 g) was dispersed in 50 cm^3 toluene by ultrasonic bath for 10 min. DETA (2 cm^3) was added and stirred at 100 °C for 30 h under N_2 atmosphere. Then, the prepared functionalized magnetic nanoparticles were separated by magnetic decantation and washed three times with ethanol to remove the unattached substrates. The resulting product was dried at room temperature.

Preparation of the Fe_3O_4–DETA–Cu(II)

In the last step, 0.25 g $Cu(NO_3)_2 \cdot 3H_2O$ was added to 0. 5 g Fe_3O_4–DETA in 30 cm^3 absolute ethanol and the resultant mixture was under reflux for 24 h. Finally, the synthesized nanosolid (Fe_3O_4–DETA–Cu(II)) was separated by magnetic decantation. The nano-magnetic catalyst washed several times with absolute ethanol, and dried under vacuum at room temperature (Scheme 1).

General procedure for the synthesis of polyhydroquinolines

A mixture of aldehyde (1 mmol), dimedone (1 mmol), ethyl acetoacetate (1 mmol), ammonium acetate (1.2 mmol) and Fe_3O_4–DETA–Cu(II) (2.25×10^{-1} mol%) was stirred at 90 °C under solvent-free conditions. Reaction progress was monitored by TLC (acetone:*n*-hexane 3:7). After completion of the reaction, the catalyst was separated using an external magnet and washed with ethyl acetate. Then, the solvent was evaporated and all products were recrystallized from ethanol. The pure polyhydroquinoline derivatives were obtained in good to excellent yields (88–98%). All the products reported here are known compounds and the spectroscopic data was matched literature values.

Acknowledgements This work was supported by the research facilities of Ilam University, Ilam, Iran.

References

1. Niknam K, Saberi D (2009) Tetrahedron Lett 50:5210
2. Liu X, Zhao X, Lu M (2015) Catal Lett 145:1549
3. Hosseini-Sarvari M, Khanivar A, Moeini F (2016) J Iran Chem Soc 13:45
4. Shiri L, Ghorbani-Choghamarani A, Kazemi M (2016) Aust J Chem 69:585
5. Shiri L, Ghorbani-Choghamarani A, Kazemi M (2016) Aust J Chem. doi:10.1071/CH16318
6. Ghorbani-Choghamarani A, Norouzi M (2014) J Mol Catal A: Chem 395:172
7. Ghorbani-Choghamarani A, Shiri L, Azadi G (2016) RSC Adv 6:32653
8. Donelson JL, Gibbs RA, De SK (2006) J Mol Catal A Chem 256:309
9. Heydari A, Khaksar S, Tajbakhsh M, Bijanzadeh HR (2009) J Fluorine Chem 130:609
10. Saha M, Pal AK (2011) Tetrahedron Lett 52:4872
11. Undale KA, Shaikh TS, Gaikwad DS, Pore DM (2011) C R Chim 14:511
12. Sirisha K, Achaiah G, Reddy VM (2010) Arch Pharm 343:342
13. Zolfigol MA, Safaiee M (2004) Synlett 827
14. Ji SJ, Jiang ZQ, Lu J, Loh TP (2004) Synlett 831
15. Sabitha G, Reddy GSKK, Reddy CS, Yadav JS (2003) Tetrahedron Lett 44:4129
16. Heravi MM, Bakhtiari K, Zadsirjan V, Saeedi M, Bamoharram FF (2010) Iran J Org Chem 2:298
17. Sapkal SB, Shelke KF, Shingate BB, Shingare MS (2009) Tetrahedron Lett 50:1754
18. Nagarapu L, Kumari MD, Kumari NV, Kantaveri S (2007) Catal Commun 8:1871
19. Reddy CS, Raghu M (2008) Ind J Chem 47:1578
20. Kumar A, Maurya RA (2008) Synlett 883
21. Ghorbani-Choghamarani A, Tahmasbi B, Moradi P, Havasi N (2016) Appl Organomet Chem 30:619
22. Rostami A, Navasi Y, Moradi D, Ghorbani-Choghamarani A (2014) Catal Commun 43:16
23. Mosaddegh E, Hassankhani A (2012) Arab J Chem 5:315
24. Surasani R, Kalita D, Dhanunjaya-Rao AV, Yarbagi K, Chandrasekhar KB (2012) J Fluorine Chem 135:91
25. Sheik-Mansoor S, Aswin K, Logaiya K, Sudhan SPN (2012) Arab J Chem. doi:10.1016/j.arabjc.2012.10.017
26. Ghorbani-Choghamarani A, Azadi G (2015) RSC Adv 5:9752
27. Das S, Santra S, Roy A, Urinda S, Majee A, Hajra A (2012) Green Chem Lett Rev 5:97
28. Raghuvanshi DS, Singh KN (2014) Ind J Chem Sect B 52B:1218
29. Kumar S, Sharma P, Kapoor KK, Hundal MS (2008) Tetrahedron 64:536
30. Mamaghani M, Kazemi-Rad R (2009) Iran J Org Chem 4:248
31. Hajjami M, Tahmasbi B (2015) RSC Adv 5:59194
32. Heravi MM, Bakhtiari K, Javadi NM, Bamoharram FF, Saeedi M (2007) J Mol Catal A Chem 264:50
33. Hong M, Cai C, Yi WB (2010) J Fluorine Chem 131:111
34. Davoodnia A, Khashi M, Tavakoli-Hoseini N (2013) Chin J Catal 34:1173